A processing pipeline and anisotropic diffusion phantom to calibrate DTI experiments

Alexandru V. Avram[1], Michal E. Komlosh[1,2], Alan S. Barnett[1,2], Elizabeth Hutchinson[1,2], Dan Benjamini[1,3], and Peter J. Basser[1]

[1]*Section on Tissue Biophysics and Biomimetics, NICHD, National Institutes of Health, Bethesda, MD, United States,* [2]*The Henry Jackson Foundation, Bethesda, MD, United States,* [3]*Department of Biomedical Engineering, Tel-Aviv University, Tel-Aviv, Israel*

Target Audience: MR scientists involved in single-subject, longitudinal and/or multicenter DTI studies

Introduction: Diffusion tensor imaging (DTI) (1) is a unique clinical tool to characterize isotropic and anisotropic water diffusion in the brain and other organs. However, the clinical quantitation of isotropic diffusion and diffusion anisotropy using DTI-derived metrics, e.g. the Fractional Anisotropy (*FA*) (2) can be biased by many experimental design and environmental factors such as gradient sampling schemes, diffusion time, diffusion pulse sequence, field strength, gradient hardware, measurement noise, etc. These can compromise the value of longitudinal data and multicenter clinical studies. There is a critical need to develop an imaging phantom based on a well-defined and known microstructure providing a broad range of diffusion anisotropy values. Here we propose the use of a novel Glass Capillary Array (GCA) phantom in conjunction with a general method for modeling the diffusion MRI signal produced by that phantom using details of the DWI pulse sequence, which employs the multiple correlation function (MCF) framework (3,4). The proposed phantom and computational methodology can be used to provide all of the standard DTI-derived parameters, including the orientationally-averaged mean diffusivity (*MD*) or mean ADC, the radial diffusivity (*RD*), eigenvalues and eigenvectors, the *FA* and other diffusion anisotropy metrics, direction-encoded color (DEC) maps, and even various types of DTI-based tractography.

Methods: Circular glass wafers containing arrays of cylindrical microcapillaries with high aspect ratios (>80:1) and different capillary diameters were filled with decamethylcyclopentasiloxation D_5 ($C_{10}H_{30}O_5Si_5$) and stacked vertically so as to allow simultaneous imaging of regions with different pore sizes within the same phantom (5). The final design consisted of six layers with three different capillary diameters (5, 10, and 25μm) as well as one layer of freely diffusing D_5 (**Fig, 1A**). DTI measurements were conducted on a 7T Bruker scanner with the 2D Spin Echo MRI sequence at 16.8 °C with temperature control. The imaging parameters are: TE/TR=58/5000ms, 1 average, FOV=16x16mm^2, and 125x125x1000μm^3 resolution, diffusion gradient pulse width δ=3ms, and separation Δ=50ms, with diffusion encoding applied along 21 directions at b=500, 2500, and 4000s/mm^2. Experimentally measured DTI metrics (DEC, *FA*, *MD*, and *RD* maps) were compared to theoretical values computed numerically using the MCF framework for diffusion in cylindrical pores (3, 4) by accounting for the amplitudes and timings of all gradient pulses in the actual experiment. The diffusivity measured in the freely diffusing D_5 layer was used in the MCF evaluation to quantify the dependence of DTI metrics on the capillary diameter in the 1-30μm range.

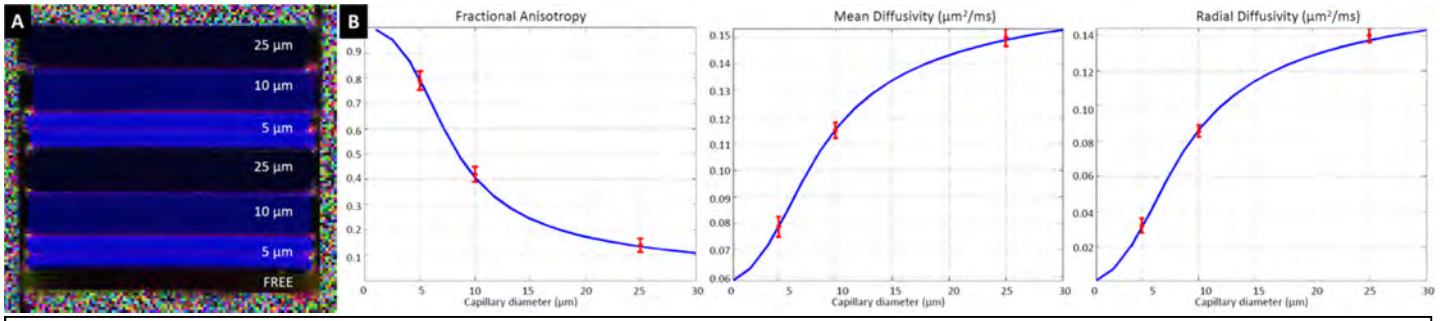

Figure 1: (**A**) *FA* modulated DEC map of cross-sectional slice through the GCA anisotropy phantom shows regions of distinct anisotropy in layers corresponding to different capillary diameters and almost zero FA in the control layer of free D_5. (**B**) Maps of DTI derived quantities (*FA*, *MD*, and *RD*) as a function of capillary diameter computed using the MCF framework (**blue**). Theoretical values are in excellent agreement with experimentally measured *FA*s (**red**). Errorbars indicate standard deviation of DTI-parameter within ROI.

Results and Discussion: The measured T_2 was 790ms and showed good homogeneity across layers with different restriction sizes, while in the freely diffusing layer of D_5 the *MD* was 0.172 μm^2/ms. These physical properties of the phantom generated excellent signal-to-noise ratio (SNR) (**Fig. 1A**) even in experiments with large b-values and/or long diffusion times for which signals in water-based phantoms can reach the noise floor, biasing the quantitation of anisotropy. DTI parameters quantified in regions-of-interest (ROIs) defined for each capillary diameter agreed remarkably well with the theoretical values for the nominal capillary diameters of 5, 10, and 25μm (**Fig. 1B**). The theoretical *FA* computed for capillary diameters in the range of 1-30 μm spans almost the entire dynamic range suggesting that this phantom is optimal for calibration of a wide range of anisotropies. Small differences between experimental and theoretical values could be attributed to measurement noise, microstructural imperfections of the GCAs, and/or susceptibility artifacts at the interfaces of adjacent wafers.

Conclusion: The low diffusivity and long T_2 as well as the well-defined cylindrical restriction-induced diffusion anisotropy make this phantom ideal for calibrating DTI measurements using many pulse sequences and experimental parameters. The current DTI phantom design can be scaled to dimensions commonly used on clinical scanners, and additional layers with different capillary orientations could be incorporated for characterizing orientational dispersion and distribution. The proposed phantom calibration methodology may improve optimization of clinical DTI protocols and remove statistical bias in longitudinal and/or multicenter clinical DTI studies. More generally, the phantom could provide a standardized diffusion MRI platform for comparing tractography algorithms, investigating mechanisms of tissue anisotropy, validating diffusion models of tissue, and quantifying restriction size (e.g. axon diameters).

References: 1. Basser et al., Biophys J 1994;66:259-267; 2. Basser & Pierpaoli, JMR 1996;111:209-219; 3. Grebenkov, Conc in Magn Res 2008;4:277-301; 4. Özarslan and Basser, J Chem Phys 2008;128:154511; 5. Komlosh et. al., JMR 2011;208:128-135;